CARBON 48 (2010) 2354–2360

available at www.sciencedirect.com

ScienceDirect

journal homepage: www.elsevier.com/locate/carbon

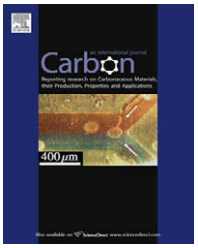

In situ observations of the nucleation and growth of atomically sharp graphene bilayer edges

Liang Qi [a], *Jian Yu Huang* [b], *Ji Feng* [a], *Ju Li* [a,*]

[a] *Department of Materials Science and Engineering, University of Pennsylvania, Philadelphia, PA 19104, USA*
[b] *Center for Integrated Nanotechnologies (CINT), Sandia National Laboratories, Albuquerque, NM 87185, USA*

ARTICLE INFO

Article history:
Received 9 December 2009
Accepted 12 March 2010
Available online 16 March 2010

ABSTRACT

Using *in situ* transmission electron microscopy, we observed the nucleation and growth of graphene bilayer edges (BLE) with "fractional nanotube"-like structure from the reaction of graphene monolayer edges (MLEs). Most BLEs showed atomically sharp zigzag or armchair crystallographic facets in contrast to the atomically rough MLEs with irregular shapes, suggesting that the BLEs are much more stable and crystallographically anisotropic. Our direct observations and theoretical studies (geometric models and *ab initio* calculations) provide important clues for tailoring the edge structure and transport properties of multi-layer graphene.

1. Introduction

Graphene is a promising new material for nano-electronics because of its high electron mobility and near-ballistic transport at room temperature [1–3]. The detailed transport properties of graphene, especially at the nanoscale, are highly sensitive to its edge terminations [4]. Most previous studies of graphene terminations have focused on monolayer edges (MLEs) [5–7]. But there tend to be a lot of defects (steps and kinks) on MLEs, which result in atomically rough edges that affect the transport properties [8–11]. The edge roughness at atomic-scale increases the variability of device behaviors [12], so it would be desirable to obtain some other graphene edge structures that are smoother and more predictable.

Recently atomically sharp graphene bilayer edges (BLEs) with "fractional nanotube"-like structures were discovered in high-resolution transmission electron microscope (HRTEM) [13–15], after high-temperature annealing. The BLEs can be thought of as being formed by a 180° low-energy elastic bending (or folding) of graphene, like the straight crease of a folded piece of paper, and have energetic stability similar to circular nanotubes (360° bending). But unlike circular nanotubes, BLEs have no rotational symmetry and posses large permanent electric dipoles [16]. They also induce interesting transport properties distinct from MLEs and circular nanotubes [16]. For the fabrication of graphene-based nano-devices, it is essential to understand the relative stability of these different types of edge terminations [15,17,18] (MLEs, BLEs, etc.) and the possible transformations between them.

In our lab, few-layer graphene has been mounted on a TEM grid and Joule-heated until sublimation of carbon into vacuum occurs. *In situ* TEM of such high-temperature heating experiments showed that although MLE-terminated holes are created on graphene initially, more than 99% of the edges end up being BLEs by the end of the experiments [15]. Thus transformations of MLE(s) to BLE(s) must have occurred [14,15], via some nucleation and growth process. We theoretically hypothesized that this transformation occurs by the reaction

$$\mathrm{MLE} + \mathrm{MLE} \rightarrow \mathrm{BLE} \tag{1}$$

with atomic-scale illustrations shown in Fig. 1. That is, when two MLEs on adjacent graphene layers cross each other, they reconstruct to form a BLE. Typically in materials kinetics

* *Corresponding author:* Fax: +1 2155 732128.
E-mail address: liju@seas.upenn.edu (J. Li).
0008-6223/$ - see front matter © 2010 Elsevier Ltd. All rights reserved.
doi:10.1016/j.carbon.2010.03.018

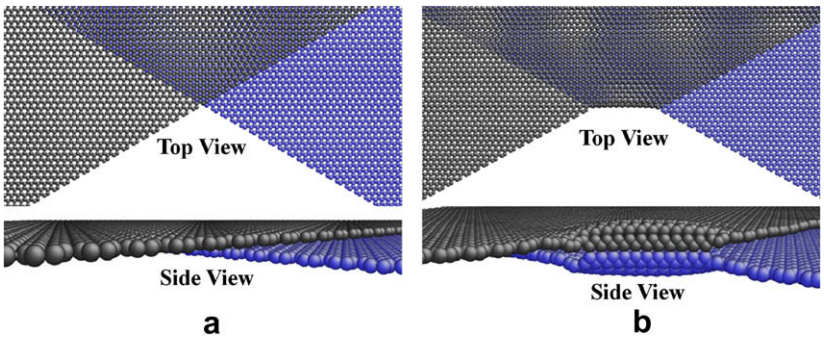

Fig. 1 – Atomic configurations of two crossing MLEs (a) and the nucleation of a BLE from them (b) as Eq. (1), where dark/light color stand for the top/bottom graphene layer.

studies, the nucleation events are very difficult to capture and characterize experimentally. Fortunately, due to the quasi-2D geometry and electron transparency of few-layer graphene, we were able to capture the BLE nucleation event and observe reaction (1) in real time.

In this paper we report *in situ* TEM observations of the nucleation and growth of BLEs from two crossing MLEs, which were initially created near the center of individual graphene by sublimation of carbon atoms, induced by Joule-heating. Our experimental results and theoretical investigations show that the BLEs are much more stable than MLEs. Furthermore, most BLEs showed clear facets on zigzag or armchair inclinations during the sublimation process, but MLEs were usually irregular in shape, indicating that BLEs have much stronger crystallographic anisotropy. In other words, BLE has a more anisotropic Wulff plot [19] than MLE. Combining *ab initio* calculations and simple geometric models, we illustrate why this may be the case. It turns out that the atomic-scale sharpness

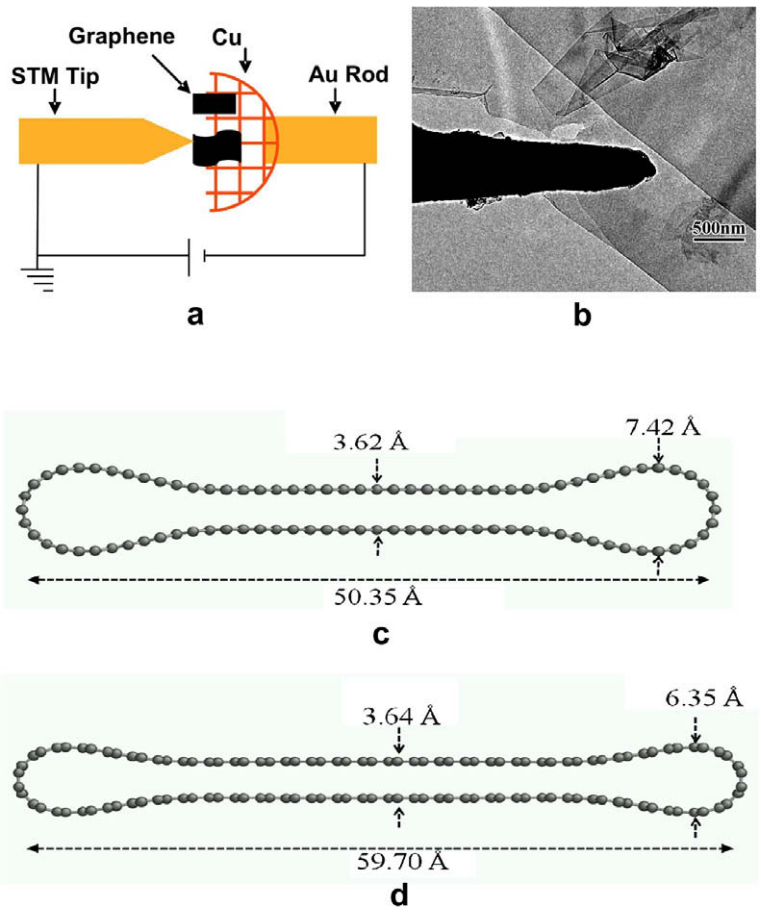

Fig. 2 – (a) Schematic of experimental setup, where a STM probe was manipulated to contact individual graphene with a layer thickness of about ten layers. (b) A TEM image showing a STM tip is contacted to graphene. (c) and (d) DFT relaxed configurations of symmetric (c) armchair and (d) zigzag BLEs.

of BLE and its strict chirality (and radius-of-curvature) selection all have a geometric origin, namely 180° folding of graphene and common lattice orientation constraint before and after folding.

2. Experimental and theoretical methods

Our *in situ* high-resolution TEM (HRTEM) observations were performed on individual graphene sheets mounted on a TEM-scanning tunneling microscopy (STM) holder. The graphene sheet was Joule-heated to high temperatures to create nanometer holes with MLEs by sublimation of carbon atoms. Graphene samples were prepared using a Scotch tape peeling method similar to that reported in the literature (Fig. 2a). Highly oriented pyrolytic graphite (HOPG) with a thickness of a few hundred microns was glued to a glass slide with a double-sided adhesive tape. The HOPG was thinned down to transparent under an optical microscope by repeated peeling using a Scotch tape. A 200 mesh TEM grid was cut into half, painted with conducting silver epoxy on the grid bars, and then glued on the transparent graphene sheet on the glass slide. Once the silver epoxy was cured, the half grid was lifted off from the glass slide. Graphene was attached to the grid after lifting off from the glass slide. The half TEM grid was glued to an Au rod of 280 μm and inserted into a Nanofactory™ TEM-STM platform, in which a fully functional STM was integrated into a TEM sample holder, allowing for *in situ* manipulation and measurements of individual graphene. TEM observations were conducted in a Tecnai F30 analytical electron microscope operated at 300 kV. A STM probe was manipulated to contact individual graphene with a layer thickness of about ten layers (Fig. 2a and b), followed by Joule-heating of the graphene to high temperatures by applying a bias voltage of about 2.5 V.

Density functional theory (DFT) calculations were performed to theoretically investigate the stability of different types of graphene edges. The calculations were performed using the Vienna *ab initio* simulation package (VASP) [20,21]. We used local density approximations (LDA) with Ceperley–Alder exchange–correlation functional [22]. Monkhorst–Pack

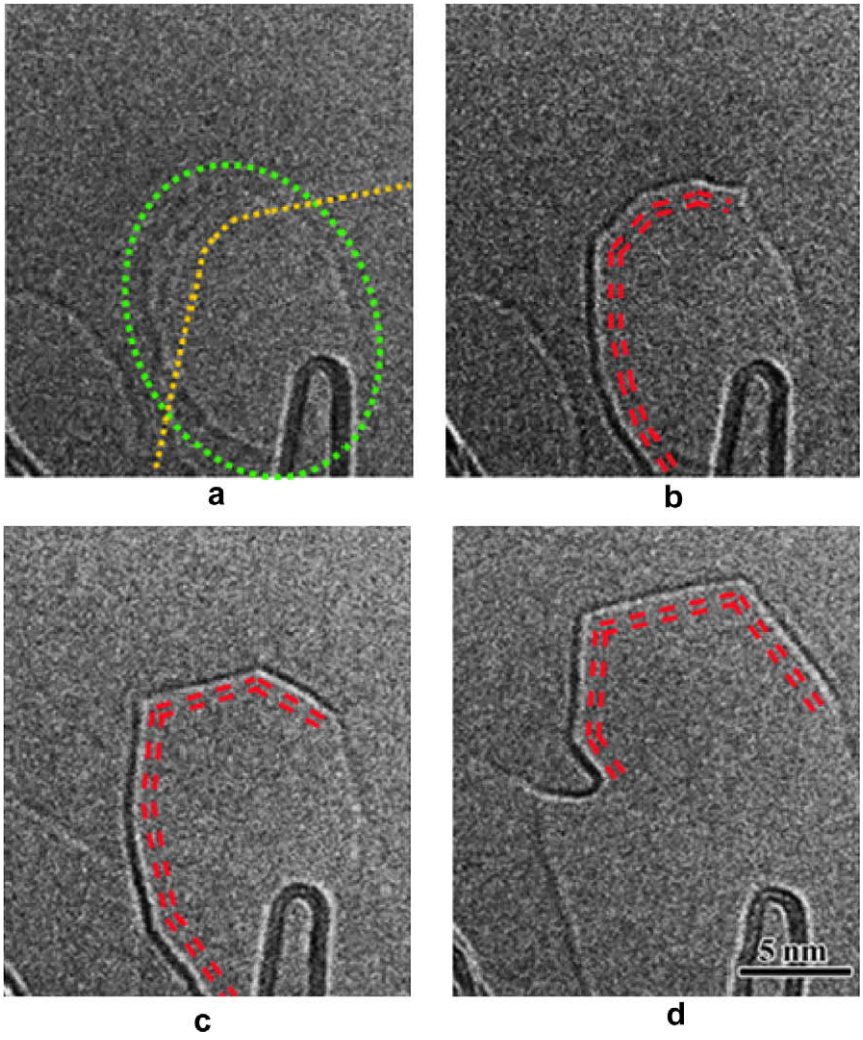

Fig. 3 – (a)–(d) Sequential HRTEM images showing BLE nucleation from crossing MLEs. Yellow- and green-dotted lines mark MLEs, and double-red-dashed lines indicate BLEs. (For interpretation of the references to color in this figure legend, the reader is referred to the web version of this article.)

k-point grids for Brillouin-zone integration were applied with **k**-point density higher than 60 per $Å^{-1}$ along a periodic direction in reciprocal space [23]. Partial occupancies of eigenstates were determined by first-order Methfessel–Paxton smearing of $\sigma = 0.1$ eV [24]. Cut-off energy for plane wave basis was 400 eV. Spin-polarization was applied to MLEs but it was found to have no effect on BLEs. The calculations were performed at equilibrium carbon bond length of 1.4094 Å. Armchair and zigzag BLEs were constructed as shown in Fig. 2c and d. There were 180 and 120 carbon atoms in the super cell for armchair and zigzag BLEs, respectively, and the corresponding width was 5.04 and 5.97 nm, respectively.

3. Results and discussions

The nucleation of BLEs from two crossing MLEs was observed by *in situ* HRTEM, as shown in Fig. 3 a–d and Movie 1 in Supporting Information. Initially elliptical or irregular (marked by green-dotted or yellow-dotted lines in Fig. 3a, respectively) shaped holes with MLEs were formed. The MLEs showed fainter contrast and expanded rapidly due to continuous atom sublimation. The holes marked in green and yellow-dotted lines were located on different graphene layers, very possibly at two neighboring layers. At a critical moment, the two crossing MLEs merged into one edge with a much darker contrast than that of a MLE, which was identified by HRTEM as an atomically sharp BLE, a "fractional nanotube" connecting two graphene layers [14,15]. These BLEs were strongly polygonized along zigzag or armchair orientations. The motions of BLEs became more sluggish compared with MLEs. Finally more than 99% of the graphene edges observed in TEM were transformed into BLEs. These nucleation and transformation reactions indicate that BLEs are much more stable than MLEs.

Density functional theory (DFT) calculations confirm the energetic advantages of BLEs. First we found in our DFT calculations that A–A rather than A–B stacking between two graphene layers ~5 nm in width, joining two symmetric BLEs (Fig. 2c and d), is the more stable configuration, consistent with recent HRTEM observations [14]. In reference to perfect monolayer graphene without edges, unreconstructed armchair and zigzag MLEs have edge energy of 1.11 and 1.36 eV/Å, respectively, and the reconstructed zigzag MLEs reduce the edge energy to 1.07 eV/Å [25]. In contrast, the excess energy of a bilayer graphene with a BLE relative to a perfect graphene bilayer without edges is only about 0.81 and 0.87 eV/Å for armchair and zigzag BLE, respectively (If a A–B stacking BLEs is considered, the excess edge energies would increase to ~1.0 eV/Å.). These results indicate that reaction (1) enjoys a gigantic energy decrease of ~1 eV/Å.

Here we provide a simple model to compute the thermodynamic driving force for the nucleation of a BLE from the crossing of two MLEs with an angle θ, as shown in Fig. 4a. If an incipient BLE segment of length c emerges at the crossing point, it would have an angle φ and $\pi - \theta - \varphi$ with the two MLEs, respectively. Also, other symmetry-equivalent BLEs with angle $\varphi \pm \pi/6$ or $\varphi \pm \pi/3$ can form. If we ignore van der Waals interaction between the two layers, the new arrangement would have an excess energy E as a function of a BLE length c. Consequently, whether or not a BLE can be nucleated depends on $dE/dc|_{c=0}$, which turns out to be

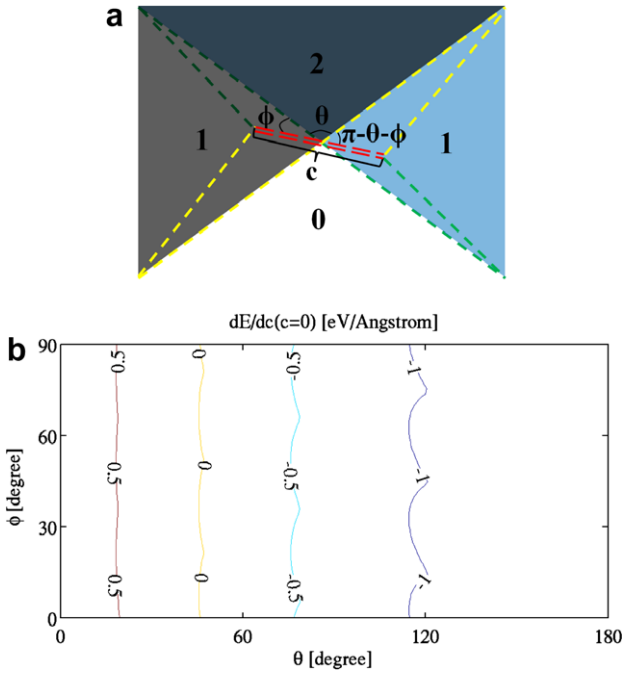

Fig. 4 – (a) Nucleating a BLE from two crossing MLEs. "0", "1" and "2" stand for the number of graphene layers in corresponding areas. θ is the angle between two crossing MLEs, and φ is the angle between the newborn BLE and one MLE. (b) The contours of $dE/dc|_{c=0}(\theta, \varphi)$, the first derivative of excess edge energy E with respect to a incipient BLE's length c at $c = 0$ for the configuration shown in (a).

$$dE/dc|_{c=0} = \gamma_2 - \gamma_1[\cos\varphi + \cos(\pi - \varphi - \theta)] \quad (2)$$

based on the geometry of the proposed reaction shown in Fig. 4a. Here γ_1 and γ_2 are the excess energy of a MLE and a BLE, respectively.

When taking $\gamma_1 = 1.10$ eV/Å and $\gamma_2 = 0.85$ eV/Å for A–A stacked BLEs, and considering the crystallographic permutations of BLEs, $dE/dc|_{c=0}$ has a much stronger dependence on θ than φ, as shown in Fig. 4b. If θ is larger than a critical value (here $\sim\pi/4$), it is always favorable to form a BLE at the crossing point, and the transformation driving force generally increases with θ (when $\theta > \pi/2$, $dE/dc|_{c=0} < -0.6$ eV/Å). If A–B stacking BLEs are used so that γ_2 increases to ~1.0 eV/Å, it would increase the critical θ value for $dE/dc|_{c=0} = 0$ from ~45° to ~55°. In the experiment, because a graphene layer is sublimated quickly after its top layer is removed, which makes the MLE at the bottom spatially close to MLE at the top layer and these two MLEs usually have a large θ with each other. For this reason, BLE nucleation can occur in most cases with two crossing MLEs.

The above addresses the coarse thermodynamic driving force for BLE nucleation. Kinetically, the nucleation occurs as carbon atoms diffuse along monolayer edges [18] and deposit onto the BLE nuclei (diffusive transformation). We suggest that monolayer edge stresses [26] and thermal fluctuations bend graphene to make an initial curved lip contact between the two layers. After nucleation, BLEs can grow by carbon diffusion, "consuming" the initially intersecting MLEs, as shown in Fig. 5a–d and Movie 2 in Supporting Infor-

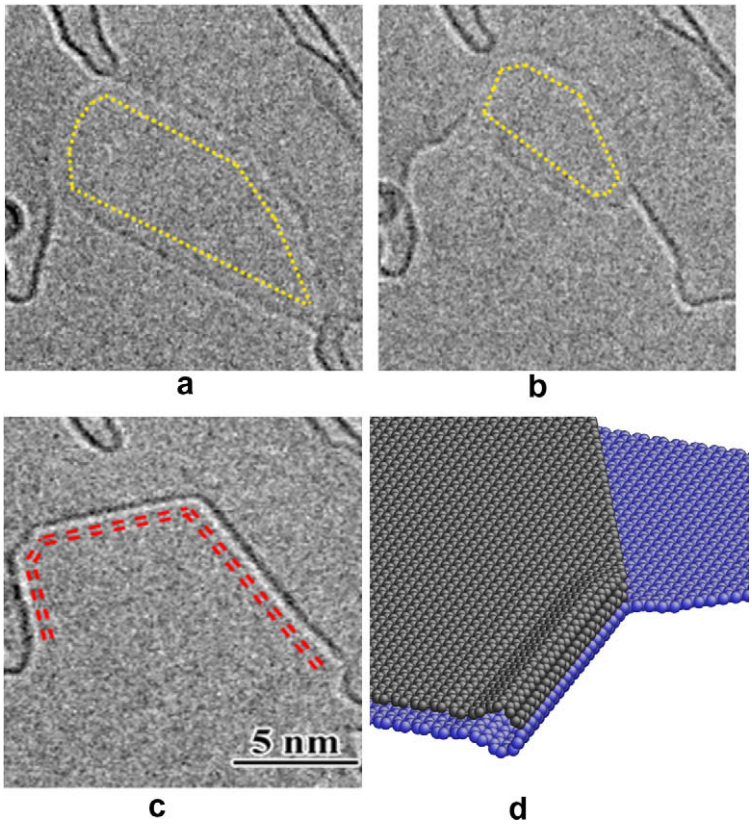

Fig. 5 – (a)–(c) Sequential HRTEM images show two MLEs zipping up to form a BLE. The single/double dashed lines stand for MLEs/BLEs. (d) Atomic configuration of a junction between two MLEs and one BLE. Dark/light color stands for atoms on top/bottom layer.

mation. Similar to Fig. 3a–d, these MLEs had irregular shapes and were sublimated quickly. At the connecting point between one BLE and two MLEs, BLE lengthened by a zipper-like reaction: two MLEs were annihilated as the BLE propagated along its original inclination (zigzag or armchair) on a straight line. In addition, similar to Movie 1, the motions of BLEs were more sluggish than those of MLEs.

The *in situ* TEM observations indicated there are significant differences in both crystallographic preference and mobility between MLEs and BLEs, suggesting that BLEs have stronger crystallographic anisotropy than MLEs. This is because zigzag and armchair inclinations are geometrically very special for BLEs. Unlike folding graphene by 360° to form chiral nanotubes, forming BLE requires 180° folding only. Generally speaking, 180° elastic folding positions the top and bottom sheets in different lattice orientations as illustrated in Fig. 6a. However, all of our graphene layers are initially of the same lattice orientation, as confirmed by electron diffraction before sublimation occurred. It is energetically impossible for a short BLE segment to alter this orientation relationship, since large twisting of one layer would be required. Therefore, the requirement that the top and bottom graphene sheets must have the same or symmetry-equivalent lattice orientations imposes an *orientation constraint* on all BLEs. Zigzag and armchair inclinations are special directions for folding BLEs because they are the only mirror-symmetry axes of graphene, folding along which satisfies the orientation constraint automatically. In these cases, only low-energy elastic bending is necessary to form the BLEs, and the hexagonal CC covalent bonding network remains intact. To satisfy the orientation constraint for BLEs of any other inclinations would require not just elastic bending, but also topological defects such as pentagons/heptagons, which compensate for the lattice orientation change due to elastic folding, like dislocations in a grain boundary. These pentagon/heptagon topological defects disrupt the hexagonal covalent bonding network, and are energetically much more expensive than elastic folding. Therefore zigzag and armchair inclinations should correspond to deep cusps in the BLE Wulff plot, under the common lattice orientation constraint. Thus the BLEs are atomically sharp crystallographic facets. Unlike carbon nanotubes (CNTs) which are poly-disperse and admit a large variety of chiralities and radii with nearly degenerate energies, the BLEs are highly mono-disperse structures for the above geometrical reasons. Not only is the chirality of a BLE fixed to be zigzag or armchair, but also its radius of curvature is completely determined by a competition between elastic bending energy and van der Waals adhesion energy between the two adjacent layers [16].

In contrast, in vacuum there always are unsaturated carbon atoms (dangling bonds) on MLEs, even the reconstructed zigzag and armchair MLEs [25], implying a weaker anisotropy in the Wulff plot. Also, because of the dangling bonds, the MLEs are chemically reactive, and upon exposure to air H,

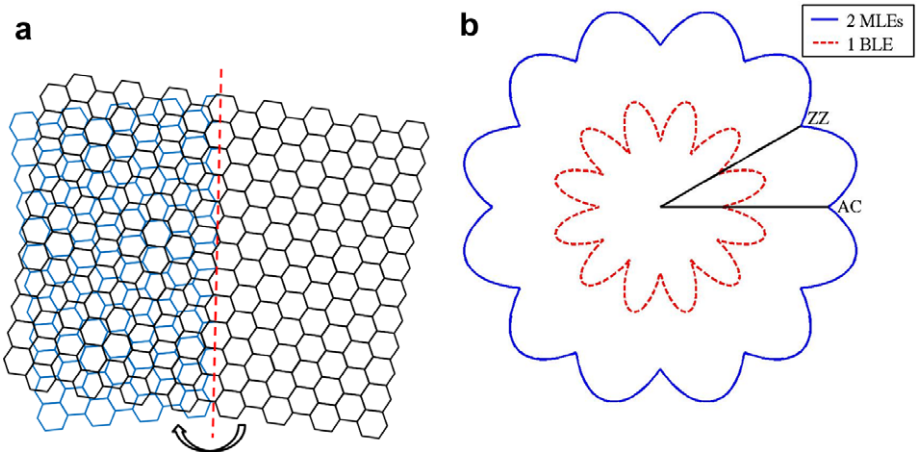

Fig. 6 – (a) Orientation change between top (dark color) and bottom (light color) graphene lattices when folding a single planar graphene sheet along an arbitrary axis, which violates the constraint that the top and bottom sheets must be of the same orientation. This orientation difference of the two layers disappears only when folding along one of the six mirror-symmetry axes (three zigzag and three armchair) of the graphene lattice. (b) Schematic illustration of Wulff plots for both 2MLEs and a BLE, which are polar plots of edge energies (radius) as functions of edge inclinations (polar angle). Here ZZ/AC stands for zigzag/armchair inclination.

O, N, etc. species could be attached on the MLEs. This chemical complexity would further increase variability in the device characteristics. The BLEs, on the other hand, have no dangling bonds, being made entirely out of carbon and are chemically inert at room temperature and in an ambient atmosphere.

Fig. 6b shows a semi-quantitative illustration of Wulff plots for both MLEs and BLEs. The relative values of edge energies for MLEs and BLEs in special inclinations (zigzag or armchair) are obtained from DFT calculations (here reconstructed zigzag MLE is used [25]). For the BLEs along general inclinations, we assume that they are composed of many zigzag/armchair BLEs segments plus edge steps, which could be adjacent pentagon–heptagon pairs as the joints connecting two CNTs with different diameters [27]. Previous calculation suggested that an adjacent pentagon–heptagon pair at such joints has defect energy of ~5 eV [28]. Because one edge step is ~2.1 Å (1.5 times of carbon bond length) along the direction perpendicular to a zigzag inclination, the edge energy of a BLE with 15° of a zigzag inclination can be estimated to be 5 eV/2.1Å × sin(15°) + 0.87 eV/Å × cos(15°) ≈ 1.46 eV/Å, much larger than those of zigzag/armchair BLEs. On the other hand, because a reconstructed zigzag MLE is fully composed of adjacent pentagon–heptagon pairs [25], the edge step on MLEs may have almost the same edge energy as the symmetrical inclinations, thus the edge energy of a MLE with 15° of a zigzag inclination is estimated to be 1.07 eV/Å × sin(15°) + 1.07 eV/Å × cos(15°) ≈ 1.31 eV/Å, confirming the much smaller differences with the symmetrical inclinations than those of BLEs.

4. Conclusions

The formation of a BLE by reaction of planar MLEs demonstrated an intermediate structure between flat carbon and curved carbon. Unlike other curved nanostructures such as fullerene and nanotubes, which are disconnected from the parent graphene, BLEs are still connected to extended graphene bilayers, with a topologically intact honeycomb lattice. From our calculations, we know that the zigzag and armchair BLEs have exceptional stabilities. Unlike MLEs which are chemically reactive and poly-disperse, the zigzag and armchair BLEs in six inclinations with exceptional stability provide us a possible avenue to make graphene-based nano-devices with stable and atomically sharp edges [29] to achieve controllable electronic properties.

Acknowledgments

This work was performed, in part, at the Center for Integrated Nanotechnologies, a US Department of Energy, Office of Basic Energy Sciences user facility. Sandia National Laboratories is a multi-program laboratory operated by Sandia Corporation, a Lockheed–Martin Company, for the US Department of Energy under Contract No. DE-AC04-94AL85000. J.L. would like to acknowledge support by NSF CMMI-0728069, Honda Research Institute USA, DOE-DE-FG02-06ER46330, AFOSR, and ONR N00014-05-1-0504.

Appendix A. Supplementary data

Supplementary data associated with this article can be found, in the online version, at doi:10.1016/j.carbon.2010.03.018.

REFERENCES

[1] Novoselov KS, Geim AK, Morozov SV, Jiang D, Katsnelson MI, Grigorieva IV, et al. Two-dimensional gas of massless Dirac fermions in graphene. Nature 2005;438(7065):197–200.

[2] Zhang YB, Tan YW, Stormer HL, Kim P. Experimental observation of the quantum Hall effect and Berry's phase in graphene. Nature 2005;438(7065):201–4.
[3] Du X, Skachko I, Barker A, Andrei EY. Approaching ballistic transport in suspended graphene. Nat Nanotechnol 2008;3(8):491–5.
[4] Neto AHC, Guinea F, Peres NMR, Novoselov KS, Geim AK. The electronic properties of graphene. Rev Mod Phys 2009;81(1):109–62.
[5] Nakada K, Fujita M, Dresselhaus G, Dresselhaus MS. Edge state in graphene ribbons: nanometer size effect and edge shape dependence. Phys Rev B 1996;54(24):17954–61.
[6] Wakabayashi K, Fujita M, Ajiki H, Sigrist M. Electronic and magnetic properties of nanographite ribbons. Phys Rev B 1999;59(12):8271–82.
[7] Son YW, Cohen ML, Louie SG. Half-metallic graphene nanoribbons. Nature 2006;444(7117):347–9.
[8] Areshkin DA, Gunlycke D, White CT. Ballistic transport in graphene nanostrips in the presence of disorder: importance of edge effects. Nano Letters 2007;7(1):204–10.
[9] Yoon Y, Guo J. Effect of edge roughness in graphene nanoribbon transistors. Appl Phys Lett 2007;91(7):073103-1–3.
[10] Sols F, Guinea F, Neto AHC. Coulomb blockade in graphene nanoribbons. Phys Rev Lett 2007;99(16):166803-1–4.
[11] Yazyev OV, Katsnelson MI. Magnetic correlations at graphene edges: basis for novel spintronics devices. Phys Rev Lett 2008;100(4):047209-1–4.
[12] Gupta AK, Russin TJ, Gutierrez HR, Eklund PC. Probing graphene edges via Raman scattering. ACS Nano 2009;3(1):45–52.
[13] Rotkin SV, Gogotsi Y. Analysis of non-planar graphitic structures: from arched edge planes of graphite crystals to nanotubes. Mater Res Innov 2002;5(5):191–200.
[14] Liu Z, Suenaga K, Harris PJF, Iijima S. Open and closed edges of graphene layers. Phys Rev Lett 2009;102(1):015501.
[15] Huang JY, Ding F, Yakobson BI, Lu P, Qi L, Li J. In-situ observation of graphene sublimation and edge reconstructions: genesis of interconnected carbon nanostructures. Proc Natl Acad Sci 2009;106:10103–8.
[16] Feng J, Qi L, Huang JY, Li J. Geometric and electronic structures of graphene bilayer edges. Phys Rev B 2009;80(16):165407-1–7.
[17] Jiao LY, Zhang L, Wang XR, Diankov G, Dai HJ. Narrow graphene nanoribbons from carbon nanotubes. Nature 2009;458(7240):877–80.
[18] Girit CO, Meyer JC, Erni R, Rossell MD, Kisielowski C, Yang L, et al. Graphene at the edge: stability and dynamics. Science 2009;323(5922):1705–8.
[19] Balluffi RW, Allen SM, Carter WC. Kinetics of materials. New York: Wiley; 2005.
[20] Kresse G, Furthmuller J. Efficiency of ab-initio total energy calculations for metals and semiconductors using a plane-wave basis set. Comput Mater Sci 1996;6(1):15–50.
[21] Kresse G, Furthmuller J. Efficient iterative schemes for ab initio total-energy calculations using a plane-wave basis set. Phys Rev B 1996;54(16):11169–86.
[22] Ceperley DM, Alder BJ. Ground-state of the electron-gas by a stochastic method. Phys Rev Lett 1980;45(7):566–9.
[23] Monkhorst HJ, Pack JD. Special points for Brillouin-zone integrations. Phys Rev B 1976;13(12):5188–92.
[24] Methfessel M, Paxton AT. High-precision sampling for Brillouin-zone integration in metals. Phys Rev B 1989;40(6):3616–21.
[25] Koskinen P, Malola S, Hakkinen H. Self-passivating edge reconstructions of graphene. Phys Rev Lett 2008;101(11):115502-1–4.
[26] Shenoy VB, Reddy CD, Ramasubramaniam A, Zhang YW. Edge-stress-induced warping of graphene sheets and nanoribbons. Phys Rev Lett 2008;101(24):245501-1–4.
[27] Charlier JC, Ebbesen TW, Lambin P. Structural and electronic properties of pentagon–heptagon pair defects in carbon nanotubes. Phys Rev B 1996;53(16):11108–13.
[28] Meunier V, Henrard L, Lambin P. Energetics of bent carbon nanotubes. Phys Rev B 1998;57(4):2586–91.
[29] Jia XT, Hofmann M, Meunier V, Sumpter BG, Campos-Delgado J, Romo-Herrera JM, et al. Controlled formation of sharp zigzag and armchair edges in graphitic nanoribbons. Science 2009;323(5922):1701–5.